USING STRONG NONLINEARITY AND HIGH-FREQUENCY VIBRATIONS TO CONTROL EFFECTIVE MECHANICAL STIFFNESS

Jon Juel Thomsen
Department of Mechanical Engineering
Technical University of Denmark
Denmark
jjt@mek.dtu.dk

Abstract

High-frequency excitation (HFE) can be used to change the effective stiffness of an elastic structure, and related quantities such as resonance frequencies, wave speed, buckling loads, and equilibrium states. There are basically two ways to do this: By using parametrical HFE (with or without nonlinearity), or by using external HFE along with strong nonlinearity. The first way has been examined for many different systems, and analytical predictions exist that has been repeatedly confirmed against numerical simulation and laboratory experiments. The current work contributes results on the other way: Combining the method of direct separation of motions with results of a modified multiple scales approach, valid also for strong or even essential nonlinearity, quantitative measures of the stiffening effect is predicted for a generic 1-dof system, and tested against numerical simulation.

Key words

High-frequency excitation; stiffening; strong nonlinearity; effective properties.

1 Introduction

Some basic aspects are explored, related to the possible use of external high-frequency excitation (HFE) and strong nonlinearity for changing the low-frequency (LF) properties of elastic structures. For a generic 1-dof model, simple analytical predictions for the effect are derived, and tested against numerical simulation results.

HFE can change various aspects of the effective properties of structures (Blekhman, 2000), but here we focus on the important *stiffening effect* (Thomsen, 2002), since a change in stiffness can change also essential system properties such as equilibrium states and stability, resonance frequencies, and frequency response.

There are at least two ways of changing effective stiffness by HFE: The first could be called *parametric stiffening*, since parametric HFE is used to change LF (or effective / average) properties; it works for linear and nonlinear systems (Blekhman, 2000; Jensen, 2000; Sorokin and Grishina, 2004; Thomsen, 2002; Fidlin, 2005; Thomsen, 2003), and is responsible for the well-known stabilization of the upside-down equilibrium of the Stephenson-Kapitza pendulum on a vibrating support (Stephenson, 1908; Kapitza, 1951). Parametric stiffening is well understood, and analytical predictions has been derived using different approximate methods (Direct Separation of Motions; Multiple Scales; Averaging), all leading to similar quantitative predictions, and agreeing with results of numerical simulation. The theoretical predictions are backed up by experimental evidence for various physical systems (Yabuno and Tsumoto, 2007; Jensen, Tcherniak and Thomsen, 2000; Thomsen, 2005; Thomsen, 2008) and references cited there.

The other way to change effective stiffness by HFE could be called *external stiffening*, since the HFE appears external to the system, as inhomogeneous HF terms in the equation of motion. For this to work the excited system must be nonlinear. Blekhman (2000; 2007) described the effect, and provided simple analytical results for calculating averaged motions and effective properties. There seems to be no published results testing the accuracy of these predictions against numerical simulation or laboratory experiments.

For external stiffening, the change in effective stiffness is predicted to be proportional to the squared HF *displacement* amplitude, and to the strength of the nonlinearity, but is independent of the HFE frequency. This contrasts to parametric stiffening, where the change in effective stiffness is proportional to the squared *velocity* amplitude of the HFE (and thus also to squared HFE frequency), and does not require nonlinearity (Thomsen, 2002).

But the strong nonlinearity needed for external stiffening imposes challenges: It may be difficult to realize, in particular with little energy loss, it complicates theoretical predictions, and it opens for many kinds of complicated and perhaps unwanted responses, with a lack of practical predictability due multiple stable states, deterministic chaos, and limited power of analytical tools. Current investigations on using external stiffening by HFE for tuning LF properties of discrete and continuous elastic waveguides are affected by these problems (Blekhman, 2007; Lazarov, Snaeland and Thomsen, 2007; Thomsen and Blekhman, 2007), and originally motivated this present work.

This work investigates the external stiffening effect in a simple setting, for a generic 1-dof model having

essential features common with the much more complicated systems mentioned above. The generic model allows for analytical predictions of strongly nonlinear LF responses, which can then be compared with results of numerical simulation and laboratory experiments.

Section 2 presents two example realizations of strongly nonlinear waveguides with HFE, and suggests a simple generic model supposed to extract an essence of these and similar systems. Section 3 presents and discusses an equation for the averaged motions of the generic model, useful for predicting effective or LF properties. Sections 4 and 5 derives simple analytical approximations for the free decay LF response (Section 4) and the LF forced frequency response (Section 5), for arbitrarily weak or strong cubic nonlinearity and strong HFE, and compares predictions to results of numerical simulation. Section 6 briefly describes current status and plans for laboratory experiments testing the theoretical predictions.

2 Two Example Systems, and a Generic Model

Ways of realizing strong nonlinearity with little energy loss may involve, e.g. lightly pre-compressed elastic beads in Hertzian contact (Daraio, et al., 2005), inherently nonlinear elastic elements such as diaphragm springs, magnets in attractive configurations with compressive linear springs in-between, and transversely loaded linear springs or strings on immovable supports. Here we exemplify models for the two latter types, and then reduce these into a common generic form for subsequent analysis.

2.1 Magnetic Nonlinearity and Linear Axial Springs

Carrella et al. (2008) suggested to use attracting magnets and repelling springs for a vibration isolating element having high-static-low-dynamic stiffness. Though close-to-linear behavior can and was achieved with such a setup, it is also possible to achieve strong or even essential nonlinearity with it. Here we consider using repetitions of one such element into a chain of oscillators.

In Figure 1, top, a one-dimensional waveguide is formed by a repeated sequence of point masses m, linear springs with stiffness k_s, and magnets (permanent or electro-) having static equilibrium separation l_s and strength K_m, with $K_m>0$ (<0) for magnets mounted in a repulsive (attractive) configuration. The equation of motion $X_j(t)$ for the jth mass can be written:

$$m\ddot{X}_j + 2k_s l_s f(X_j/l_s) = P(X_{j-1,\,j,\,j+1}, \dot{X}_{j-1,\,j,\,j+1}, t), \quad (1)$$

where overdots denote time derivatives, f is the non-dimensional restoring force function, here representing spring and magnet forces due to a displacement X_j when $X_{j-1}=X_{j+1}=0$, and P collects all forces on m other than those represented by the left-hand side, i.e. damping forces, spring and magnet forces occurring when the adjacent masses are not at rest, and external forces.

The restoring function f can be calculated using the inverse-square law for magnetic attraction or repulsion between a pair of magnets, i.e. force=K_m/(separation)^2, where K_m is proportional to permeability and pole strengths (for electromagnets proportional to electric current squared); this gives:

$$f(x) = x\left(1+\tfrac{1}{2}\mu(1-x^2)^{-2}\right); \quad \mu = 2K_m/k_s l_s^{\,3}, \quad (2)$$

where $x = X_j/l_s$, $|x|<1$, and μ represents the magnet-to-spring strength, positive (negative) for repulsive (attractive) magnet configurations. The Taylor-expansion about the static equilibrium $x=0$ is:

$$f(x) = \kappa x + \gamma x^3 + O(x^5), \quad (3)$$

where κ represents linear stiffness, and γ the coefficient of the dominating nonlinearity:

$$\kappa = 1+\tfrac{1}{2}\mu, \quad \gamma = \mu. \quad (4)$$

Figure 1, bottom, illustrates f for $x\in[0;1]$, while the antisymmetric part $f(-x) = -f(x)$ for $x\in[-1;0]$ is omitted. It appears that qualitatively different restoring force characteristics can be realized, though when $\kappa\le 0$ only with negative cubical stiffness γ. In the present context also configurations of negative or vanishing stiffness are of interest, since even if $\kappa\le 0$, HFE may add enough positive effective stiffness to stabilize $x=0$.

2.2 Axial and Transverse Linear Springs Combined

Transverse spring elements for creating nonlinearity have been considered in various contexts related to vibration damping, canceling, or isolation using e.g. piano wire or rubber bands (Dohnal, Paradeiser and Ecker, 2006; Carrella, Brennan and Waters, 2007; Miranda and Thomsen, 1998; Kerschena, et al., 2007).

The waveguide in Figure 2, top, has axial linear springs of stiffness k_s, and nonlinearity is provided by linear springs with stiffness k_t mounted transversely to the direction of axial motions of the pointmasses. The unloaded length of each transverse springs is l_{t0}, while in the static equilibrium shown in the figure, with the springs orthogonal to the longitudinal axis, each spring is pre-stretched the distance $\Delta l_{t0} > -l_{t0}$ to length $l_t = l_{t0} + \Delta l_{t0}$. The initial equilibrium stretch of axial springs is

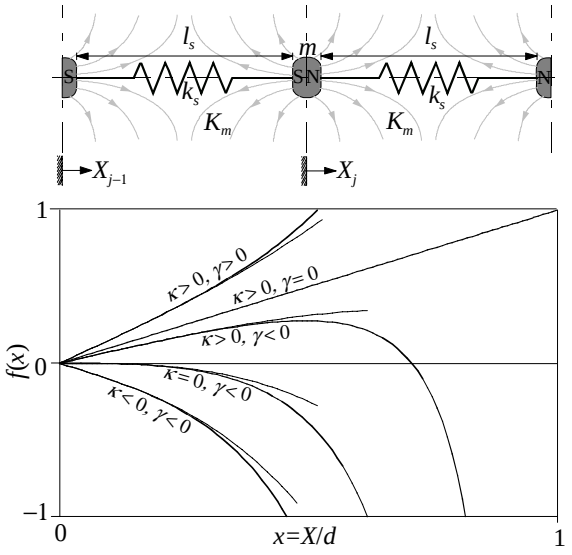

Figure 1. Top: Example physical realization of strong elastic nonlinearity in a waveguide using magnets and linear springs. Bottom: Realizable types of force-displacement characteristics $f(x)$, according to (2) (thick, solid line), and a 3rd-order Taylor expansion (3), with κ and γ characterizing linear and cubical stiffness, respectively.

irrelevant in this formulation.

In this case the equation of motion for the *j*th mass is:

$$m\ddot{X}_j + 2k_s l_{t0} f(X_j/l_{t0}) = P(X_{j-1,j,j+1}, \dot{X}_{j-1,j,j+1}, t), \quad (5)$$

where P is defined as for (1), while the nondimensional restoring force becomes:

$$f(x) = x\left(1+\hat{k}_t\left(1-\left(x^2+(1+\delta^2)\right)^{-1/2}\right)\right), \quad (6)$$

where $x = X_j/l_{t0}$, and $\delta = \Delta l_{t0}/l_{t0} > -1$ is the relative pre-stretch (if $\Delta l_{t0}>0$) or pre-compression (if $\Delta l_{t0}<0$) of the transverse springs, and $\hat{k}_t = k_t/k_s$ is the transverse-to-axial linear spring stiffness. The Taylor expansion is again (3), but now with linear stiffness and cubical coefficient, respectively, instead of (4):

$$\kappa = 1+\hat{k}_t\left(1-(1+\delta)^{-1}\right), \quad \gamma = \tfrac{1}{2}\hat{k}_t(1+\delta)^{-3}. \quad (7)$$

Figure 2, bottom, shows qualitatively different restoring force characteristics for positive x, with the antisymmetric part for $x<0$ omitted. Due to the restriction $\delta > -1$, a negative cubical coefficient γ cannot be achieved, while all other combinations of negative or positive or vanishing linear and cubical restoring force is possible. In particular an essentially nonlinear ($\kappa/\gamma = 0$) or strongly nonlinear $\left|\kappa/\gamma x_{\max}^2\right| \ll 1$ restoring force with positive cubical coefficient can be obtained, since $\kappa = 0$ while $\gamma \neq 0$ results when $\delta = -(1+\hat{k}_t)^{-1}$, i.e. with suitably precompressed transverse springs. Also, if the masses are magnetic, the features of the systems in Figure 1 and Figure 2 combine, and any combination of positive, negative, or vanishing linear and nonlinear stiffness coefficients can be realized.

2.3 A Generic 1-DOF Model

While Lazarov et al. (2007) and Thomsen & Blekhman (2007) considers the effective properties of HF-excited discrete multi-DOF and continuous systems, respectively, this present work aims at shedding more light on the basic effect of strong nonlinearity combined with HFE, detached from the extra complexity associated with many degrees of freedom. Thus we model the dynamics of just one of the masses in Figure 1 or Figure 2, neglecting the interaction with adjacent masses by considering their motions explicitly given, e.g. as part of the functions P in (1) and (5). Motions are rescaled to be $O(1)$, and time is rescaled such that the normalized linear stiffness coefficient, if present, has unit magnitude. As a generic representation of the functions P, we choose a combination of a linear dissipative term, and explicit LF and HF terms, the latter time-harmonic. This defines a generic model for a strongly nonlinear 1-dof oscillator with strong HFE:

$$\ddot{x} + 2\zeta\dot{x} + kx + \gamma g(x) = q(t) + \Omega^2 A(t)\sin(\Omega t),$$
$$x = x(t),\ (x(0),\dot{x}(0)) = (x_0, v_0),\ 0 < \zeta \ll 1, \quad (8)$$
$$k \in \{-1,0,+1\},\ \gamma \in \mathbb{R},\ \Omega >> 1,\ (x,g,A) = O(1),$$

where k gives the sign (or lack of presence) of the linear stiffness term, the function g is essentially nonlinear (i.e. $g(0) = dg/dx|_{x=0} = 0$) and its coefficient γ can be arbitrarily large, Ω is the HFE frequency and $A(t)$ its (possibly slowly varying) displacement amplitude, and $q(t)$ is the LF excitation (LFE). A characteristic of this system, compared to the other HFE systems mentioned in the introduction, is the presence of strong ($\left|k/\gamma x_{\max}^2\right| \ll 1$) or essential ($k/\gamma = 0$) nonlinearity.

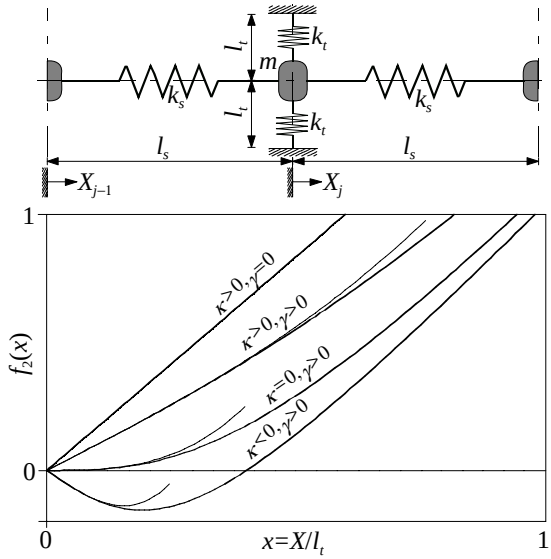

Figure 2. Top: Another realization of strong, elastic nonlinearity, here using transverse linear springs. Bottom: Realizable types of force-displacement characteristics $f(x)$, according to (6) (thick, solid line), and a 3rd-order Taylor expansion (3) with κ and γ characterizing linear and cubical stiffness, respectively, as defined in Sect. 2.2

3 Predicting Effective Properties and LF Responses for the Generic System

3.1 Averaged System

Aiming at predicting average / effective / LF system properties, i.e. as observed after low-pass filtering $x(t)$ with a cut-off frequency less than Ω, we use the Method of Direct Separation of Motions (Blekhman, 2000; Fidlin, 2005; Thomsen, 2005) to split the unknown motions into slow and fast components z and ψ:

$$x = x(t,\tau) = z(t) + \psi(t,\tau), \quad \tau = \Omega t, \quad \langle\psi\rangle = 0, \quad (9)$$

where τ is the "fast time", considered a new independent variable along with the "slow time" t, angle brackets denote fast-time average over one HFE period $\tau \in [0;2\pi]$ with t considered constant, and the constraint of the fast motions ψ having zero fast time average implies that $\langle x\rangle = z(t)$, so that "slow motions" z are defined as the fast-time average of the full motions x.

To determine the fast motions ψ, substitute (9) into (8), noting that $d/dt = \partial/\partial t + \Omega\partial/\partial\tau$, and solve for ψ to lowest order in the small parameter Ω^{-1} to obtain the so-called *inertial approximation*:

$$\psi(t,\tau) = -A(t)\sin\tau + O(\Omega^{-1}), \quad (10)$$

Then average (8) (with (9) substituted), and obtain the equation for the slow motions z:

$$\ddot{z} + 2\zeta\dot{z} + kz + \gamma\langle g(x+\psi)\rangle = q(t),$$
$$(z(0),\dot{z}(0)) = (x_0, v_0 + \Omega A(0)), \quad (11)$$

which is exact if ψ is exact, or neglects small terms of order Ω^{-1} if (10) is used for ψ.

The results (9)-(11) have been reported by Blekhman (2000; 2007), using the same method. Also, Fidlin (2000) and (2005) (p.284), using a multiple scales method for the case of "very strong excitation", derived averaged equations for a system which includes (8) as a special case; Using his general results for (8), one obtains also (9)-(11).

The assumption $A = O(1)$ in (8), along with (10), implies the fast motions ψ are $O(1)$, and thus not necessarily small. This contrasts many other studies of HFE effects. For the present case, with only external HFE, an assumption of A and ψ being small would show changes in effective system properties only at ignorable higher order.

3.2 Case of Interest: Polynomial Restoring Force

Equation (11) holds for any nonlinear function $g(x)$. In many relevant cases the physical restoring force can be adequately represented by a third order Taylor series, so that $g(x) = x^3 + \beta x^2$. With this and (10) inserted, the averaged system (11) becomes:

$$\ddot{z} + 2\zeta\dot{z} + \bar{\omega}_0^{\,2}(t)z + \gamma(z^3 + \beta z^2) = q(t) + \bar{g}_0(t),$$
$$\bar{\omega}_0^{\,2}(t) = k + \tfrac{3}{2}\gamma A(t)^2, \quad \bar{g}_0(t) = -\tfrac{1}{2}\beta A(t)^2, \qquad (12)$$
$$\big(z(0), \dot{z}(0)\big) = \big(x_0, v_0 + \Omega A(0)\big).$$

This models a nonlinear oscillator very similar to the original one (8), though, with an additional explicit excitation term $\bar{g}_0$ depending on slow time only, and an effective linear stiffness coefficient $\bar{\omega}_0^{\,2}$, generally varying in slow time if the excitation amplitude A is not constant. So, the average effect of the external HFE is LF-parametric in character, with an additional external LF-component in the asymmetric case $\beta \neq 0$.

3.3 Effective Stiffness and Bias

If A is constant, it appears from (12), then $\bar{\omega}_0^{\,2}$ is the effective static stiffness, which can be smaller or larger than the "true" (structural) stiffness k, and also change in sign, dependent on the sign of the nonlinear coefficient γ. Stronger nonlinearity provides a larger change in stiffness, and if the physical restoring force is essentially nonlinear ($k/\gamma = 0$), then all effective linear stiffness comes from γA^2, i.e. from nonlinearity combined with HFE. While γ is usually fixed by the physical configuration, the HFE amplitude A can be readily changed, so that effective structural stiffness – according to (12) – can be controlled in (slow) time on demand. To quantify an example: A ±10% change in effective linear natural frequency $\bar{\omega}_0$ requires $\gamma = O(0.1)$, supposing $k = 1$ and recalling that $A = O(1)$.

If the physical restoring force is purely antisymmetric wrt. $x = 0$, then $\beta = 0$, and to the order of approximation used with (12), the only average effect of HFE is to change the effective linear stiffness. But any asymmetry in the physical restoring force ($\beta \neq 0$) will be reflected as an inhomogeneous term $\bar{g}_0$ in (12), biasing the average response away from $z = 0$. If A is (quasi-)constant, this term is also (quasi-)constant, and the effect of the HFE then appears similar to a (quasi-)static external force. To first order, i.e. for a relatively weak bias effect, the equilibrium $z = 0$ (for $\beta = 0$) is then displaced to $z = \bar{g}_0 / \bar{\omega}_0^{\,2} = -\beta / (2kA^{-2} + 3\gamma)$. This provides a means for controlling equilibrium position by (slow) variation of the HFE amplitude A.

The coefficients $\bar{\omega}_0^{\,2}$ and $\bar{g}_0$ do not depend on Ω, and thus the linear stiffening and biasing effect of external HFE with strong nonlinearity seems independent of the HFE frequency. This contrasts the case of *parametric* stiffening by HFE, where the change in linear stiffness is proportional to $(\Omega A)^2$ (and independent of nonlinearity) (Thomsen, 2002). But for both cases the results assumes $\Omega \gg 1$, and as Ω decreases from a large value, the accuracy and even qualitative correctness can be expected to drop.

Next we consider the case of symmetric restoring force ($\beta = 0$), and solve the averaged equation (12) approximately for two important cases: "Free LF response" (Section 4), and "LF near-resonant response" (Section 5).

4 Free LF response: Frequency-Amplitude relation for $g(x) = x^3$

The analysis of the "free response" (i.e. with only HFE) is important because it provides the basic nonlinear relationship between LF oscillation frequency and amplitude, and in particular how this changes with external HFE. Furthermore, the frequency-amplitude curve forms the backbone of the corresponding nonlinear LF *forced* response (cf. Section 5), i.e. the curves of stationary LF vibration amplitude versus LFE frequency, in the presence of external HFE.

Thus we consider the response of the generic system (8) for a linear plus purely cubic restoring force when there is no damping and no slow external forcing, the unforced equilibrium is (marginally) stable, and the HFE has constant amplitude, i.e. $\beta = \zeta = q = \dot{A} = 0$, $k \geq 0$; Then (9)-(10) and (12) gives:

$$x(t) = z(t) - A\sin(\Omega t) + O(\Omega^{-1}), \qquad (13)$$
$$\ddot{z} + \omega_0^{\,2} z + \gamma z^3 = 0, \quad \omega_0^{\,2} = k + \tfrac{3}{2}\gamma A^2. \qquad (14)$$

where if $\gamma < 0$ we require $k = 1$ and $A^2 < -2/3\gamma$ so that $\omega_0^{\,2} > 0$ and $z = 0$ is (marginally) stable to small disturbances.

4.1 Analytical Prediction

Equation (14) for the averaged motions is an autonomous Duffing equation, whose oscillation frequency ω as a function of oscillation amplitude a can be expressed by a complete elliptic integral (Polyanin and Zaitsev, 2003). But this does not apply to more general forms of g, and therefore we prefer to use a series solution in terms of elementary functions, given by Burton and Hamdan (1983). They used a nonlinear time transformation method, which will work under mild restrictions on $g(x)$, and for the current choice of $g = x^3$ gives a frequency-amplitude relation $\omega(a)$ that can be written as (Burton and Hamdan, 1983):

$$\omega = \frac{\sqrt{\omega_0^{\,2} + \tfrac{3}{4}\gamma a^2}}{\sum_{j=0}^{\infty} D_{2j}\tilde{\varepsilon}^{2j}}, \quad \tilde{\varepsilon} = \frac{\gamma a^2}{4\omega_0^{\,2} + 3\gamma a^2}, \qquad (15)$$
$$D_{2j} = (4j)^{-2}(4j-1)(4j-3)D_{2j-2}, \quad D_0 = 1.$$

where ω_0^2 is defined in (14).

In (15) the sequence D_{2j} is quickly decreasing with j. Also, when $\gamma \geq 0$ then $|\tilde{\varepsilon}| < \frac{1}{3}$, and the series term for ω converges rapidly towards the exact elliptic integral solution, regardless of the strength γa^2 of the nonlinearity; Even the first term ($j = 0$) may give an acceptable approximation, i.e. $\omega \approx \sqrt{\omega_0^2 + \frac{3}{4}\gamma a^2}$. Taylor-expanding this for the special case of small γa^2, one finds $\omega \approx \omega_0 + \frac{3}{8}\gamma a^2/\omega_0$, which is identical to what is obtained by the method of multiple scales for the weakly nonlinear Duffing oscillator (Thomsen, 2003).

When $\gamma < 0$ then $\omega_0^2 > 0$ requires $k = 1$ and $A^2 < -2/3\gamma$. Also, $|\tilde{\varepsilon}| < \frac{1}{3}$ (and quick convergence of ω in (15)) is not guarantied, but requires $a^2 < -2/3\gamma - A^2$.

4.2 Testing Against Numerical Simulation

Figure 3 depicts the frequency-amplitude relation, $a(\omega)$ as predicted by (15), for cases ranging from linear ($\gamma = 0$) over weakly nonlinear to strongly nonlinear ($\gamma = 50$), and further details given in the legend. Each curve tells the frequency at which the system will oscillate freely, if released with a given amplitude. In the absence of HFE (dashed lines), increased nonlinearity just results in the well-known bend over of the response curve towards higher frequencies (for $\gamma > 0$), with the low-amplitude root of all curves remaining at the linear natural frequency (here unity). In the presence of HFE (solid lines), these curves are shifted upward in frequency, i.e. the system appears effectively stiffened, and this stiffening grows with the strength γa^2 of the nonlinearity. The HFE also appears to *soften* nonlinearity: With HFE the system is effectively less nonlinear than without, as appears from the high-amplitude part of the dashed curves being closer to straight lines (this actually signals strong nonlinearity, as $\omega \to \sqrt{\frac{3}{4}\gamma}a$ for a large nonlinearity γa^2; cf. (15)) than their corresponding curves in solid line; most pronounced for the curves corresponding to the strongest nonlinearity, $\gamma = 10$ and $\gamma = 50$.

As appears (circle markers), the averaged response of numerical simulations (using the MATLAB ODE-solver ODE45) of the full system (8) follows the approximate, analytical predictions (15) quite closely, even for the cases of strongest nonlinearity. The main factor affecting the goodness of fit is not the strength of the nonlinearity, but the magnitude of the excitation frequency Ω: If, for example, the value of Ω=100 used for the figure is doubled, the numerical simulation results for the strongest nonlinearity ($\gamma = 50$) fits even better. However, decreasing Ω to e.g. the value 50, the simulated response ends up at frequencies 10-20% from the predicted value. This and other observed cases of discrepancy may be explained, at least partly, by the HFE exciting a nonlinear resonance, i.e. the response ends up at a stable part of the underlying forced frequency response, rather than oscillating at its (nonlinear) natural frequency. The strong bend and reach of the free-response backbones in Figure 3 into frequencies much higher than the linear natural frequency (here unity) illustrates, that the condition $\Omega \gg 1$ is insufficient to ensure good accuracy of averaged predictions like (15); the main condition is that the HFE must not excite fast motions much larger than the assumed magnitude order, $O(1)$.

Figure 4 shows a typical numerically simulated free-response (except for the HFE) time series for a moderately strong nonlinearity $\gamma = 10$, mild damping, and otherwise the same conditions as for Figure 3. For the upper trace there is no HFE, and the damped nonlinear response $x(t)$ decays with a visibly decreasing frequency, which approaches the linear natural frequency of unity (i.e. oscillation period 2π) for small amplitudes. The lower trace shows (in black line) $x(t)$ for the case of HFE with $A = 1$ and $\Omega = 50$, along with the fast-time average $\langle x(t) \rangle$ (in white line). While the fast component of motion remains, as the HFE, it appears the averaged or slow motions decay, and while decaying their frequency increases towards the value 4 (oscillation period $\pi/2$), which is also the value predicted using (15). Thus the system is effectively stiffened, i.e. it appears so if the full response x is averaged or low-pass filtered. Then one can control the LF oscillation frequency of the system simply by changing the HFE amplitude A.

5 LF Harmonic forcing: LF Frequency response-force for $g(x) = x^3$

Next we consider the possible LF or averaged response of the generic system (8) in the presence of

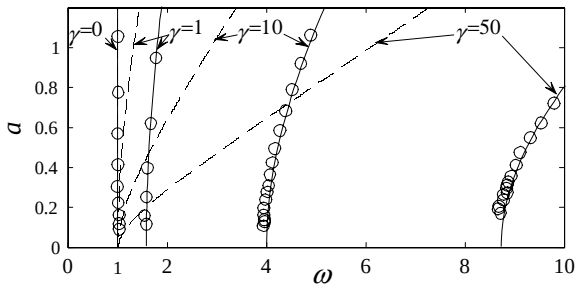

Figure 3. Frequency-amplitude relation $a(\omega)$ for free oscillations of the nonlinear oscillator (8) with $g(x) = x^3$, $k = 1$, $q = \zeta = 0$, $\Omega = 100$, and $A = 1$ (solid line) or $A = 0$ (dashed). Lines: As predicted by the approximate expression (15) (using 2 terms in the series, but the plotted results appear identical when using ≥1 terms). Circles: Numerical simulation of (8), averaged over periods $2\pi/\Omega$ of the high-frequency excitation. Cases shown: Linear ($\gamma = 0$), and weakly ($\gamma = 1$), moderately ($\gamma = 10$), and strongly nonlinear ($\gamma = 50$).

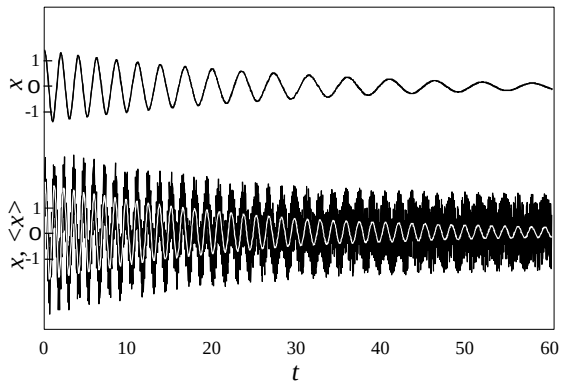

Figure 4. Numerically simulated time response of the nonlinear oscillator (8) with $g(x) = x^3$, $k = 1$, $\gamma = 10$, $q = v_0 = 0$, $\zeta = 0.05$, $\Omega = 50$, $x_0 = 1.2$. Upper time trace: Response $x(t)$ in the absence of HFE (A=0); Lower trace: Response $x(t)$ in the presence of HFE ($A = 1$), and its running fast-time average $\langle x \rangle = z$ (in white line).

arbitrarily weak or strong cubical nonlinearity, weak damping, arbitrarily strong or weak harmonic LFE, and stationary HFE. Thus $\beta = \dot{A} = 0$, $k \geq 0$, $q(t) = q_0 \sin(\Omega_0 t)$, $\gamma \in \mathbb{R}$, $0 < \zeta \ll 1$, and (9)-(10), (12) gives:

$$x(t) = z(t) - A\sin(\Omega t) + O(\Omega^{-1}), \tag{16}$$

$$\ddot{z} + 2\zeta\dot{z} + \omega_0^2 z + \gamma z^3 = q_0 \sin(\Omega_0 t), \tag{17}$$

$$\omega_0^2 = k + \tfrac{3}{2}\gamma A^2, \tag{18}$$

where $\Omega_0 = O(\omega_0)$ is the frequency of the LFE and q_0 its constant amplitude, $\omega_0 \ll \Omega$ is the effective linear natural frequency, and if $\gamma < 0$, we require $k = 1$ and $A^2 < -2/3\gamma$ so that $\omega_0^2 > 0$ and $z = 0$ is (marginally) stable to small disturbances.

5.1 Analytical prediction

Burton & Rahman (1986), using a modified version of the method of multiple scales, derived approximate analytical expressions for the stationary frequency response of a Duffing oscillator with arbitrarily weak or strong nonlinearity. Their results are readily applicable to the averaged system (17), after transforming into a new time variable $\hat{t} = \omega_0 t$. Then Eq. (27) in Burton & Rahman (1986) gives the following stationary solution, in terms of our present parameters:

$$\begin{aligned} z(t) &= a_0 \sin(\Omega_0 t + \phi_0) \\ &\quad + \tfrac{1}{8}\tilde{\varepsilon}_0 a_0 \sin\left(3(\Omega_0 t + \phi_0)\right) + O(\tilde{\varepsilon}_0^{\,2}), \end{aligned} \tag{19}$$

where $\tilde{\varepsilon}_0$ is the expansion parameter:

$$\tilde{\varepsilon}_0 = \frac{\gamma a_0^{\,2}}{4\omega_0^2 + 3\gamma a_0^{\,2}} \tag{20}$$

and the stationary amplitude a_0 of the fundamental harmonic in (19) is given as solutions of the following algebraic frequency response equation (corresponding to Eq. (26) in Burton & Rahman (1986)):

$$\Omega_0^{\,2} = \omega_0^2 + \tfrac{3}{4}\gamma a_0^{\,2} \pm \sqrt{(q_0/a_0)^2 - (2\zeta\Omega_0)^2}. \tag{21}$$

The solutions a_0 to (21) correspond to stable solutions (19) of (17), *unless* a value for Ω_0 gives three possible solutions for a_0; then the solution corresponding to the middle amplitude is unstable. The backbone of the frequency response is obtained by letting $q_0 = \zeta = 0$ in (21), i.e. $\Omega_0^{\,2} = \omega_0^2 + \tfrac{3}{4}\gamma a_0^{\,2}$, which is identical to the (strongly dominating) first term of the series expansion (15) for the free response $\omega = \omega(a)$.

In the *weakly nonlinear* case one has $\gamma a_0^{\,2}/\omega_0^2 \to 0$ and $\tilde{\varepsilon}_0 \to \tfrac{1}{4}\gamma a_0^{\,2}/\omega_0^2$, and (19) reduces to the well-known perturbation solution for a weakly nonlinear Duffing oscillator excited near primary resonance (e.g. Burton & Rahman (1986); Thomsen (2003)).

However, it follows from (20) that as the strength $\gamma a_0^{\,2}$ of the nonlinearity grows from zero (linear case) to infinity (essentially nonlinear case), then $\tilde{\varepsilon}_0$ grows monotonically from zero to 1/3; even with an essential nonlinearity ($\omega_0^2 = 0$ or $\gamma a_0^{\,2}/\omega_0^2 \to \infty$) the value of $\tilde{\varepsilon}_0$ is limited to 1/3. Hence the approximation (19), in terms of an expansion in $\tilde{\varepsilon}_0$, does not break down even for *strong nonlinearity*; in fact it follows from (19)-(20), that following a resonance curve from the low-amplitude linear part ($\tilde{\varepsilon}_0 \approx 0$) to the high-amplitude and/or strongly nonlinear part ($\tilde{\varepsilon}_0 \to 1/3$), the amplitude of the 3rd harmonic changes from close to zero to at most 1/24 of the fundamental harmonic.

The reason for the lack of breakdown of the approximation for strong nonlinearity lies in the manner Burton & Rahman (1986) modifies the standard version of the multiple scales perturbation method to give (19)-(21): With the standard multiple scales approach one uses an expansion parameter ε which is proportional to the strength of the nonlinearity, and a detuning parameter $\varepsilon\sigma$ to express the nearness of the excitation frequency to the linear natural frequency, i.e. to the linear frequency response backbone. Both ε and $\varepsilon\sigma$ should be small, and this is naturally not fulfilled at strongly nonlinear resonance. Burton & Rahman (1986) instead uses an expansion parameter $\tilde{\varepsilon}_0$ which occurs naturally in a series expansion for the nonlinear backbone (i.e. free response) curve; cf. the similar definitions of $\tilde{\varepsilon}$ and $\tilde{\varepsilon}_0$ in (15) and (20), and then use a detuning parameter $\tilde{\varepsilon}_0\tilde{\sigma}$ to express the nearness of the stationary response to the *nonlinear* backbone. This means that both the expansion parameter and the detuning remains small at every level of nonlinearity, and thus that (19)-(21) adequately approximates all stationary responses that are not to far from the approximation to the the nonlinear backbone.

To illustrate the frequency responses we solve (21) for the squared LFE frequency $\Omega_0^{\,2}$ and obtain:

$$\begin{aligned} \Omega_0^{\,2} &= \omega_0^2 + \tfrac{3}{4}\gamma a_0^{\,2} - 2\zeta^2 \\ &\quad \pm \sqrt{(q_0/a_0)^2 - 4\zeta^2(\omega_0^2 + \tfrac{3}{4}\gamma a_0^{\,2} - \zeta^2)}, \end{aligned} \tag{22}$$

which for the case of *weak damping* gives:

$$\begin{aligned} \Omega_0 &= \left(1 \mp \zeta^2 a_0/q_0\right)\sqrt{\omega_0^2 + \tfrac{3}{4}\gamma a_0^{\,2} \pm q_0/a_0} \\ &\quad + O(\zeta^4), \quad \text{for} \quad 0 < \zeta \ll 1. \end{aligned} \tag{23}$$

We then define the predicted LF stationary vibration amplitude a as the sum of the two lowest harmonic amplitudes, i.e. by (19):

$$a = (1 + \tfrac{1}{8}\tilde{\varepsilon}_0)a_0. \tag{24}$$

Equations (19)-(24) allows for qualitative and quantitative prediction of some essential features of external HFE.

Figure 5 shows two typical frequency responses $a(\Omega_0)$ as predicted by (24) and (22) (or (23); there is no discernible difference for the parameters used), with solid (dashed) line denoting stable (unstable) solutions, and with parameters as given in the legend. For Figure (a) there is no HFE, and the strength of the nonlinearity at resonance is large enough ($\gamma a_0^{\,2} = O(10)$) to produce a pronouncedly bent resonance peak, with a backbone that emanates from the linear natural frequency at unity, and becomes almost a straight line for the highest amplitudes.

For Figure 5(b) HFE has been added, at a frequency Ω one hundred times the linear, unforced natural frequency ω_0. As a consequence, it appears, the effective LF frequency response moves towards higher frequencies, and becomes "less nonlinear": The backbone for the LF resonance curve now emanates from a frequency ω_0 four times higher than the linear unforced natural frequency, reflecting the average stiffening effect of the HFE, and the resonance spike has less

overhang and is more curved, reflecting that the increase in effective linear stiffness makes nonlinearity less pronounced.

5.2 Testing Against Numerical Simulation

In Figure 5, circle markers show the averaged response of numerical simulations (see technical details at the end of this section) of the full system (8); as appears these agree very well with the approximate analytical predictions. Again, as in Section 4.2, the main factor affecting the goodness of fit is not the strength of the nonlinearity, but the magnitude of the excitation frequency Ω, which should be large compared to the resonance frequency.

In Figure 6, the upper plot shows part of a stationary time series $x(t)$ as obtained by numerical simulation with LFE frequency $\Omega_0=4$, and other parameters as for Figure 5. The response $x(t)$ has the same frequency as the input, and a low amplitude of 0.067, as predicted also theoretically (cf. the value of a in Figure 5(a) for $\Omega_0 = 4$). The lower time trace in Figure 6 shows (in black line) $x(t)$ when HFE is added ($\Omega=100$). The output oscillates at both the HFE and LFE frequencies, and since the HFE input amplitude is large ($A=1$), the HFE output amplitude is also large. More interestingly, the HF- averaged output $\langle x(t)\rangle$ (white line), which oscillates at the LFE frequency, also has a high value amplitude, of 0.55, as predicted also theoretically (cf. the value of a in Figure 5(b) for $\Omega_0=4$). This illustrates how HFE and strong nonlinearity can substantially change the LF resonance properties of the system: Without HFE, the LFE at $\Omega_0 = 4$ is somewhat above resonance for the particular system, while *with* HFE the same LFE is effectively resonant.

Figure 7 shows a pair of LF frequency responses similar to Figure 5, i.e. without and with HFE, but for

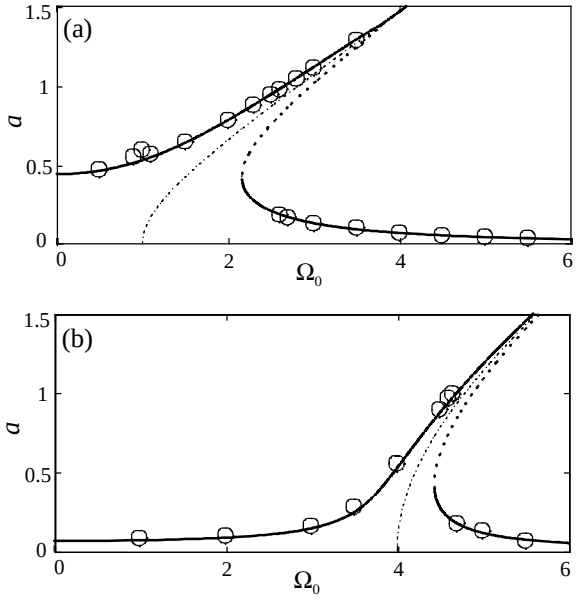

Figure 5. LF frequency response $a(\Omega_0)$ for LF and HF forced oscillations of the nonlinear oscillator (8) with $g(x)=x^3$, $k=1$, $\gamma=10$, $q(t)=q_0\sin(\Omega_0 t)$, $q_0=1$, $\zeta=0.05$, $\Omega=100$, $(x_0,v_0)=(0.01,0)$ (typically; see text), and (a) *without* HFE ($A=0$); (b) *with* HFE ($A=1$). Solid / dashed line: Stable / unstable solution according to the theoretical prediction (24) with (22); Circles: Numerical simulation of (8), averaged over periods $2\pi/\Omega$ of the high-frequency excitation.

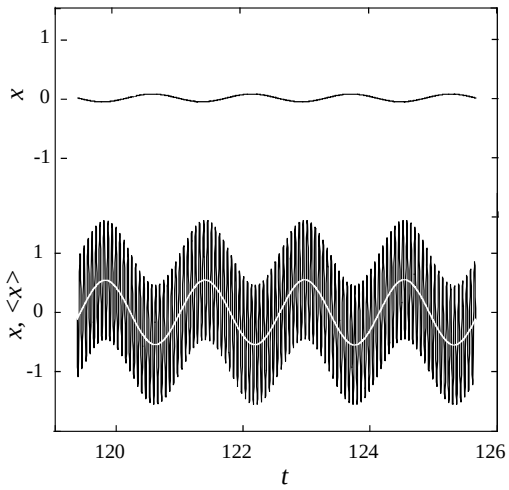

Figure 6. Numerically simulated time response of the nonlinear oscillator (8). Upper time trace: Response $x(t)$ in the absence of HFE, but LF excitation at $\Omega_0 = 4$; Lower trace: Response $x(t)$ when HFE is added, and its running fast-time average $\langle x\rangle=z$ (in white line). Parameters as for Figure 5.

the case of *essential nonlinearity* ($k=0$). This causes the backbone of the system without HFE (Fig. (a)) to be a straight but non-vertical line ($a_0=\sqrt{\frac{4}{3}}\Omega_0/\gamma$, cf. (22) with $\omega_0^2=\zeta=q=0$), i.e. there is no "preferred" or natural oscillation frequency which is independent of oscillation amplitude. In Figure (b) HFE has been added, and this makes the (averaged) system behave close to linearly at low amplitudes: There is an effective natural frequency $\omega_0=\sqrt{\frac{3}{2}\gamma}=3.87$ (cf. (18)), from which the backbone emanates vertically, while only at higher amplitudes the hardening nonlinearity bends the response curve towards higher frequencies. This exemplifies how HFE might be used to effectively tune the LF properties of systems: With an essential structural nonlinearity, all effective linearity comes from the HFE, so that the natural frequency can be adjusted over a wide range of frequencies down to

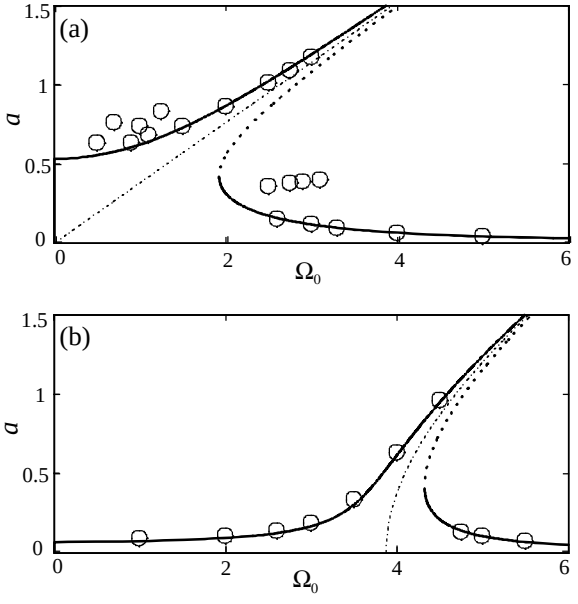

Figure 7. LF frequency response as Figure 5, but with essential nonlinearity ($k=0$; other parameters unchanged). (a) *without* HFE ($A=0$); (b) *with* HFE ($A=1$).

zero. For Figure (b) very good agreement between analytical predictions (lines) and numerical simulation(circles) is noted. For Figure (a) most of the numerical simulation points fall closely on the predicted curve, while there are some outliers that need more consideration to be explained than is possible here.

The above numerical results were generated using MATLAB's ODE-solver ODE45 to simulate (8) for times long enough for stationarity in the solution $x(t)$ to evolve. Then the running average $\langle x(t) \rangle$ of the post-transient part of $x(t)$ was computed, using the HFE period $2\pi/\Omega$ as the averaging window size, and the amplitude of $\langle x(t) \rangle$ was calculated. Initial conditions (x_0,v_0) were as given in the figure legend, except for some of the values of Ω_0 where two solutions for a_0 are predicted; in these cases the default initial conditions typically gave stationary solutions on the low-amplitude part of the resonance curve, while solutions on the upper overhanging part of the curve was reached by using, as initial conditions, an arbitrary pair $(x(t),\dot{x}(t))$ for a stationary solution already obtained on the upper part, but for a slightly different value of Ω_0 (this is similar to performing a very slow sweep in LFE frequency in a lab.-experiment).

6 Experimental testing

At the time of writing an experimental setup for testing the theoretical predictions of sections 4 and 5 is almost ready; testing will begin soon, and the results reported separately.

The experimental device consists of a vertical rigid bar, simply supported by a roller bearing in one end, and supported in the other by a length of piano or guitar string with adjustable pre-tension, i.e. essentially a single cell of Figure 2, with $k_s=0$ and $k_t=EA/l_{t0}$, where EA is longitudinal string stiffness. With zero string pre-tension the restoring force for the rigid bar is essentially cubic, while structural linearity can be added by tensioning the string. Controlled and measurable HFE and LFE is provided by a vibration shaker, which connects to the bar via a stinger and a force transducer. The output response is measured by an accelerometer mounted on the bar or a laser displacement sensor.

To test the predictions of Section 4, HFE will be applied to the bar. When stationarity has been established, the bar will be tapped using an instrumented hammer, and the free decay LF response recorded and processed (e.g. averaged over the HF period); this should give results comparable to Figure 3 and Figure 4.

The predictions of Section 5 will be tested by using classical LF up-down sweeps at a very low sweep rate, allowing stationarity to be established before recording the stationary LF and HF amplitudes; this should give results comparable to Figure 5, Figure 6, and Figure 7.

7 Conclusions

Simple analytical predictions for the nonlinear LF frequency-amplitude relations of a generic system with external HFE and arbitrarily weak or strong nonlinearity has been presented. Substantial changes in effective (LF) stiffness and frequency response are predicted. In particular, with a cubical hardening nonlinearity the effective linear natural frequency shifts to higher frequencies, and the nonlinear features of the LF resonance curve becomes less pronounced. It should be stressed that these changes in effective behavior is a consequence solely of changing the external HFE, i.e. by "turning a knob", while the real physical system properties (inertia, restoring force, and damping) are unchanged.

The approximate analytical method involves two steps: The first is a separation of full motions into LF and HF components, of which the latter here is only interesting by their effect on LF motions. The next step is to attack the resulting strongly nonlinear equation for the LF motions using a modified method of multiple scales that can handle arbitrarily weak or strong polynomial nonlinearity. The result of the combined procedure is approximate analytical expressions for both HF and LF components of motions, along with expressions for the LF frequency response curves and backbones.

For the cases tested, the agreement between analytical predictions and results of numerical simulation is generally very good, as long as the underlying assumptions are fulfilled, that is: The HFE frequency should be much larger than the LF resonance frequencies of the system (i.e. linear resonance as well as primary and possible secondary nonlinear resonances), and the stationary LF motions should be periodic and, if strongly nonlinear, then be close to the (nonlinear) backbone for the unforced and undamped system.

It should be recalled that the good agreement mentioned above not necessarily implies good "practical" predictability for real systems: With strong nonlinearity involved, several stationary solutions may coexist and be stable for a given set of parameters, and the one actually reached depends on initial conditions. This not only means that e.g. two different stable periodic motions may exist for the same LFE frequency (as demonstrated in Section 5), but also that other stable motions may exist that will not be revealed by the above procedure, e.g., chaotic motions or possible motions with a frequency-amplitude combination far from the backbone of primary LFE resonance. The latter include super- and subharmonic resonance, and (for multi-DOF systems) internal resonance.

Laboratory experiments are currently being initiated to test the predictions of the present work. Also, several theoretical issues seems relevant to pursue, such as consideration to transient LF response (e.g. to impulse input), softening nonlinearity ($\gamma < 0$), initially unstable structural equilibrium ($k<0$), multi-DOF systems, and secondary nonlinear resonances (super/subharmonic and internal resonance).

Acknowledgement

This work was supported by grant 274-05-0498 from the Danish Research Council for Technology and Production Sciences.

References

Blekhman, I. I. (2000). Vibrational Mechanics - Nonlinear Dynamic Effects, General Approach, Applications World Scientific, Singapore.

Blekhman, I. I. (2007). On vibratory dynamic materials and composites. Doklady Physics **52**(6), 335-338.

Burton, T. D. & Hamdan, M. N. (1983). Analysis of non-linear autonomous conservative oscillators by a time transformation method. Journal of Sound and Vibration **87**(4), 543-554.

Burton, T. D. & Rahman, Z. (1986). On the multi-scale analysis of strongly non-linear forced oscillators. International Journal of Non-linear Mechanics **21**(2), 135-146.

Carrella, A., Brennan, M. J., & Waters, T. P. (2007). Static analysis of a passive vibration isolator with quasi-zero-stiffness characteristic. Journal of Sound and Vibration **301**, 678-689.

Carrella, A., Brennan, M. J., Waters, T. P., & Shin, K. (2008). On the design of a high-static-low-dynamic-stiffness isolator using linear mechanical springs and magnets. Journal of Sound and Vibration **In Press**(Available online 5 March), (22 pp.).

Daraio, C., Nesterenko, V. F., Herbold, E. B., & Jin, S. (2005). Strongly nonlinear waves in a chain of Teflon beads. Physical Review E **72**(1), 1-9.

Dohnal, F., Paradeiser, W., & Ecker, H. (2006). Experimental study on cancelling self-excited vibrations by parametric excitation, In Proceedings of IMECE 2006, Paper ID IMECE2006-14552., International Mechanical Engineering Congress & Exposition (IMECE2006) ASME, Chicago, USA; 5-10 Nov. 2006 pp. 10 pages

Fidlin, A. (2000). On asymptotic properties of systems with strong and very strong high-frequency excitation. Journal of sound and vibration **235**(2), 219-233.

Fidlin, A. (2005). Nonlinear Oscillations in Mechanical Engineering Springer-Verlag, Berlin Heidelberg.

Jensen, J. S. (2000). Buckling of an elastic beam with added high-frequency excitation. International Journal of Non-Linear Mechanics **35**(2), 217-227.

Jensen, J. S., Tcherniak, D. M., & Thomsen, J. J. (2000). Stiffening effects of high-frequency excitation: experiments for an axially loaded beam. ASME Journal of Applied Mechanics **67**(2), 397-402.

Kapitza, P. L. (1951). Dynamic stability of a pendulum with an oscillating point of suspension (in Russian). Zurnal Eksperimental'noj i Teoreticeskoj Fiziki **21**(5), 588-597.

Kerschena, G., McFarland, D. M., Kowtko, J. J., Lee, Y. S., Bergman, L. A., & Vakakis, A. F. (2007). Experimental demonstration of transient resonance capture in a system of two coupled oscillators with essential stiffness nonlinearity. Journal of Sound and Vibration **299**(4-5), 822-838.

Lazarov, B., Snaeland, S. O., & Thomsen, J. J. (2007). Using strong nonlinearity and high-frequency vibrations to control effective properties of discrete elastic waveguides, In A. L. Fradkov et al. (ed.)., Proceedings of the Sixth EUROMECH Nonlinear Dynamics Conference, June 30 - July 4, 2008, St. Petersburg, Russia IPME, Russian Academy of Sciences, St. Petersburg, Russia pp. 6 pages

Miranda, E. C. & Thomsen, J. J. (1998). Vibration induced sliding: theory and experiment for a beam with a spring-loaded mass. Nonlinear Dynamics **16**(2), 167-186.

Polyanin, A. D. & Zaitsev, V. F. (2003). Handbook of Exact Solutions for Ordinary Differential Equations (2nd Ed.) Chapman & Hall/CRC, Boca Raton, Florida.

Sorokin, S. V. & Grishina, S. V. (2004). Analysis of wave propagation in sandwich beams with parametric stiffness modulations. Journal of Sound and Vibration **271**(3-5), 1063-1082.

Stephenson, A. (1908). On a new type of dynamic stability. Memoirs and Proceedings of the Manchester Literary and Philosophical Society **52**(8), 1-10.

Thomsen, J. J. (2002). Some general effects of strong high-frequency excitation: stiffening, biasing, and smoothening. Journal of Sound and Vibration **253**(4), 807-831.

Thomsen, J. J. (2003). Vibrations and Stability: Advanced Theory, Analysis, and Tools Springer-Verlag, Berlin Heidelberg.

Thomsen, J. J. (2005). Slow high-frequency effects in mechanics: problems, solutions, potentials. International Journal of Bifurcation and Chaos **15**(9), 2799-2818.

Thomsen, J. J. (2008). Effective properties of mechanical systems under high-frequency excitation at multiple frequencies. Journal of Sound and Vibration **311**(3-5), 1249-1270.

Thomsen, J. J. & Blekhman, I. I. (2007). Using nonlinearity and spatiotemporal property modulation to control effective structural properties: dynamic rods, In M. Papadrakakis et al. (ed.), CD-ROM Proceedings of COMPDYN2007 (ECCOMAS Thematic Conference on Computational Methods in Structural Dynamics and Earthquake Engineering), 13-16 June 2007, Rethymno, Crete, Greece. National Technical University of Athens, Rethymno, Crete, Greece pp. 12 pp.

Yabuno, H. & Tsumoto, K. (2007). Experimental investigation of a buckled beam under high-frequency excitation. Archive of Applied Mechanics **77**(5), 339-351.